

EDITORIAL | AUGUST 16 2024

## Special topic on Wide- and ultrawide-bandgap electronic semiconductor devices **FREE**

Special Collection: [Wide- and Ultrawide-Bandgap Electronic Semiconductor Devices](#)

Joachim Würfl ; Tomás Palacios ; Huili Grace Xing ; Yue Hao ; Mathias Schubert  



*Appl. Phys. Lett.* 125, 070401 (2024)

<https://doi.org/10.1063/5.0221783>



### Articles You May Be Interested In

Ultrawide bandgap semiconductors

*Appl. Phys. Lett.* (May 2021)

We are 60!

*Appl. Phys. Lett.* (September 2022)

To boldly go: New frontiers for APL

*Appl. Phys. Lett.* (August 2020)

16 September 2025 19:18:20

## Instruments for Advanced Science

- Knowledge
- Experience
- Expertise

Click to view our product catalogue

Contact Hiden Analytical for further details:

[www.HidenAnalytical.com](http://www.HidenAnalytical.com)

[info@hiden.co.uk](mailto:info@hiden.co.uk)

### Gas Analysis

- dynamic measurement of reaction gas streams
- catalysis and thermal analysis
- molecular beam studies
- dissolved species probes
- fermentation, environmental and ecological studies

### Surface Science


- UHV-TPD
- SIMS
- end point detection in ion beam etch
- elemental imaging - surface mapping

### Plasma Diagnostics

- plasma source characterization
- etch and deposition process reaction kinetic studies
- analysis of neutral and radical species

### Vacuum Analysis

- partial pressure measurement and control of process gases
- reactive sputter process control
- vacuum diagnostics
- vacuum coating process monitoring



# Special topic on Wide- and ultrawide-bandgap electronic semiconductor devices

Cite as: Appl. Phys. Lett. **125**, 070401 (2024); doi: [10.1063/5.0221783](https://doi.org/10.1063/5.0221783)

Submitted: 3 June 2024 · Accepted: 15 June 2024 ·

Published Online: 16 August 2024



View Online



Export Citation



CrossMark

Joachim Würfl,<sup>1</sup> Tomás Palacios,<sup>2</sup> Huili Grace Xing,<sup>3</sup> Yue Hao,<sup>4</sup> and Mathias Schubert<sup>5,a)</sup>

## AFFILIATIONS

<sup>1</sup>Ferdinand-Braun-Institut GmbH (FBH), Gustav-Kirchhoff-Straße 4, 12489 Berlin, Germany

<sup>2</sup>Massachusetts Institute of Technology (MIT), 77 Massachusetts Avenue, RM 39-567A, Cambridge, Massachusetts 02139, USA

<sup>3</sup>College of Engineering, Cornell University, Ithaca, New York 14850, USA and Institute of Materials and Systems for Sustainability, Nagoya University, Nagoya 464-8601, Japan

<sup>4</sup>State Key Discipline Laboratory of Wide Band-Gap Semiconductor Technology, School of Microelectronics, Xidian University, Xi'an 710071, People's Republic of China

<sup>5</sup>University of Nebraska-Lincoln, Lincoln, Nebraska 68588-0511, USA and NanoLund, Lund University, P.O. Box 118, 22100 Lund, Sweden

**Note:** This paper is part of the APL Special Collection on Wide- and Ultrawide-Bandgap Electronic Semiconductor Devices.

<sup>a)</sup>Author to whom correspondence should be addressed: [mschubert4@unl.edu](mailto:mschubert4@unl.edu)

<https://doi.org/10.1063/5.0221783>

Despite the tremendous progress on wide-bandgap materials in the last few decades, devices made of these materials are still far from their maximum theoretical performance, especially at high frequencies and voltage levels. At the same time, new ultrawide-bandgap materials have the potential to improve this performance even further, but a better understanding of mobile carrier dynamics, charge transport, electron-hole recombination, and interaction with charged defects in dependence on specific operation conditions and mission profiles is needed, including supporting modeling and simulation. This collection of papers summarizes recent progress on some of the key wide and ultra-wide bandgap semiconductor technologies, including GaN, AlGaIn, AlN, Ga<sub>2</sub>O<sub>3</sub>, BN, and diamond for rf and power applications, as well as photonic devices. More general papers on new characterization techniques and radiation effects in semiconductors are also included as they are of general interest for all wide bandgap semiconductor device developers. The following paragraphs provide an overview on the major topics of (1) GaN based devices and materials, (2) gallium oxide devices and technologies, (3) novel wide bandgap materials, (4) diamond, (5) photonics, and (6) notable characterization methods covered by the current collection of papers on “Wide- and ultrawide-bandgap electronic semiconductor devices.”

GaN based devices are becoming more mature nowadays and are commercially available, especially lateral devices for rf and power electronic applications. Despite this success, the performance of these devices is still far from their theoretical limit. The paragraphs below on GaN power, rf, and exploratory GaN and AlN-based devices summarize the main papers trying to address these issues.

In terms of GaN power devices, several papers focus on improving lateral normally off power transistors based on p-GaN gate technology.

Park *et al.* from Samsung Advanced Institute of Technology demonstrated a new passivation technique based on N<sub>2</sub>O plasma treatment of the access region being of lateral p-GaN gated high electron mobility transistors (HEMTs).<sup>1</sup> This creates an oxygen-rich GaON/AlGaON compound layer and, thus, reduces device dispersion and improves reliability.

Optical deep level transient spectroscopy investigations of the minority carrier (electron) traps in Schottky type p-GaN gate high electron mobility transistors were reported by Chen *et al.* of ShanghaiTech University.<sup>2</sup> Activation energy, capture cross section, and trap concentration of three different traps were identified.

Lee *et al.* of the Massachusetts Institute of Technology optimized the cross-sectional geometry of p-GaN gated lateral power transistors and demonstrated the impact of engineering the relative dimension of the gate metal and the p-GaN structure.<sup>3</sup> This will provide new degrees of design freedom for device engineers.

According to Rahman *et al.* from Ohio State University, the use of high k material, such as BaTO<sub>3</sub> encapsulating the gate electrode, can increase the break-down voltage and bring them closer to their theoretical limits.<sup>4</sup> The technique allows for extremely compact devices with respect to their gate-drain distance and, thus, very efficient power switches at given voltage levels.

Shima *et al.* from Tohoku University adds another important feature to the portfolio of lateral and vertical GaN transistor designs: the

technology toward the realization of laterally defined p-type regions by ion implantation and subsequent activation process.<sup>5</sup> Their work focuses on an effective vacancy-guided redistribution and activation process after sequentially implanting  $Mg^+$  and  $N^+$  ions. This allows for atmospheric post implantation damage annealing and, thus, reduces process complexity.

Several papers focus on vertical GaN devices, such as Schottky and pn-diodes and GaN based vertical trench metal-oxide-semiconductor field-effect transistors (MOSFETs).

Liao *et al.* of Tohoku University report on low-leakage nanorod Schottky diodes on native GaN substrates achieving breakdown levels around 800 V.<sup>6</sup>

Nomoto *et al.* from Cornell University compared distributed polarization-doped pn-diodes against impurity doped GaN pn-diodes and demonstrate impressive performance in polarization-doped devices.<sup>7</sup> Polarization doping in this case is achieved by employing AlGaIn layers with a linearly graded Al composition between 0% and 7% resulting in a coherently strained AlGaIn region.

A complete quasi-vertical trench MOSFET fabricated on sapphire wafers employing an epi stack with a step graded channel structure has been demonstrated by Zhu *et al.* from Hong Kong University of Science and Technology.<sup>8</sup> The use of a step-graded channel doping improves the trade-off between maximum device current, on-state resistance, and positive threshold voltage.

Shih *et al.* from the Massachusetts Institute of Technology reported on their digital wet etching technology that allows for low damage high aspect ratio nanometer-scale vertical etching in GaN/AlGaIn based materials.<sup>9</sup> The paper offers interesting process modules for improving fabrication processes for many different GaN and AlGaIn devices.

Defect detection, characterization, and engineering are keys for further developing power devices for fast and reliable switching applications.

In a paper highlighted by the APL editors, DasGupta *et al.* from Sandia National Laboratory analyzed defect states in GaN epitaxial layers for vertical power switching pn-diodes.<sup>10</sup> The authors identified a defect state 0.6 eV below the conduction band that is responsible for high voltage and high temperature leakage of these devices.

The analysis of gate insulator properties on differently etched GaN structures is important for further developing vertical GaN trench MOSFETs and other devices. Mukherjee *et al.* from the University of Padua compared the effect of planar etching treatment and trench formation on the performance of GaN-based MOS using stacked  $SiO_2/Al_2O_3$  dielectric layers on n-doped epitaxial layers of GaN.<sup>11</sup> In this way, the authors mimicked the dielectric gate oxide properties on the vertical sidewall geometry present in actual GaN trench MOSFETs.

The tri-gate FET concept proposed by Nela *et al.* of the Ecole Polytechnique Federale de Lausanne can serve as another very promising approach toward reducing on-state resistance of power electronic devices at a given drain voltage.<sup>12</sup> This paper proposes a monolithic integration of a normally off Tri-gate transistor that is in a cascade configuration with a normally on GaN high voltage transistor. Such configuration would enable ultra-low on-state resistance values combined with high breakdown. This technology combines processing techniques for lateral GaN based devices with techniques characteristic for vertical GaN devices, such as trench etching and the sidewall deposition of an optimized gate oxide. Depending on the geometry of the

multichannel trenches, such devices can be designed for normally off behavior.

GaN rf-devices can be significantly boosted by reducing parasitic elements, such as source and drain Ohmic contacts resistances. Zhou *et al.* in Xidian University show a concept on how to optimize mm-wave GaN based transistors by using regrown Ohmic contact structures on innovative epitaxial stacks, such as InAlN barriers combined with AlN spacers on the GaN channel layer.<sup>13</sup> These regrown contacts feature contact ledges on the source and the drain side contact that take over rf-conductivity at mm-wave frequencies.

Wang *et al.* from Xidian University demonstrated significant power level and power added efficiency improvements for millimeter-wave GaN HEMTs with a 60 nm gate technology by combining an ultrathin AlGaIn barrier concept with a 2 nm *in situ* SiNx gate dielectric and a carefully designed slanted gate field plate.<sup>14</sup> This approach significantly reduced short channel effects, cut down drain and gate lagging effects, and thus, resulted in mm-wave devices with a highly balanced trade-off between breakdown voltage and speed.

Ye *et al.* at the University of Notre Dame explore ultra-wideband AlGaIn channel FETs for high-power rf-application.<sup>15</sup> These devices feature a thin AlGaIn channel with high-Al content of 45% placed between AlGaIn barrier layers with Al concentration of 62%. This results in devices with high specific breakdown strength, comparably linear transfer characteristics, and a very modest temperature dependence.

High power GaN p-type/i-type/n-type (PIN) diodes are interesting for a variety of high-power switching applications. Thus, the noise characteristics of such elements is an important parameter. Ghosh *et al.* from the University of California, Riverside, investigated low noise performance of such devices and characterized the 1/f dependency on device operation current.<sup>16</sup>

The devices considered in this section either employ new wide bandgap materials, electron and hole conduction schemes, or gate drive concepts. All these features are important to either provide complementary logic approaches with wide bandgap devices, to have more efficient gate drivers, to explore new material systems, such as AlN based devices, or to provide new processing modules for the above-mentioned concepts.

Zhang *et al.* from Cornell University reported on the growth of pseudomorphic GaN/AlN heterostructures on AlN crystals by using molecular beam epitaxy.<sup>17</sup> The authors created a p-type conductive channel region at the GaN/AlN interface. The obtained large hole mobility of 280  $Vs/cm^2$  is assumed to be the result of the low defect density of the layers grown on native AlN substrate. These results provide a baseline toward efficient p-type devices fabricated in the GaN/AlN material system.

Defect-assisted hole conductivity in N-polar AlGaIn/GaN superlattices grown by molecular beam epitaxy on Si was reported by Krishna *et al.* from University of California, Santa Barbara.<sup>18</sup>

Another approach toward p-type channel GaN FETs for complementary logic applications has been reported by Zheng *et al.* from Hong Kong University of Science and Technology.<sup>19</sup> The authors demonstrated a buried p-type channel FET using oxygen treatment of the recessed p-GaN region before gate oxide deposition. Depending on the actual shape of the vertical band diagram underneath the gate, a parasitic two-dimensional electron gas (2DEG) channel can be generated at the AlGaIn/GaN interface. Although this channel is not directly

connected to the p-GaN device, it influences device performance and has been investigated thoroughly to find the proper top p-type channel device operation conditions for minimizing its effect.

According to the investigations by Su *et al.* from Xidian University, the dislocation density of p-GaN layers for p-type channel GaN MOSFETs is decisive for the quality of the p-type Ohmic contacts.<sup>20</sup> They found that oxygen annealed Ni/Au p-type Ohmic contacts on GaN layers grown on patterned sapphire substrates are superior to the same contacts on p-GaN grown on non-structured conventional sapphire. This knowledge can be used to further improve the quality of p-type channel GaN devices.

Transistors with Al-rich AlGaN channel are expected to show a high Johnsons and Baliga's figure of merit. The breakdown voltage of Al-rich ternary compounds reaches very large values of 17 MV/cm for pure AlN material. Khachariya *et al.* from North Carolina State University, Raleigh designed and fabricated such kind of devices and reported a breakdown field of 11.5 MV/cm in undoped Al<sub>0.55</sub>GaN test structures.<sup>21</sup>

In another paper, Khachariya *et al.* from North Carolina State University, Raleigh investigated Schottky contacts fabricated on N-polar GaN for high temperature applications.<sup>22</sup> A thin low-pressure chemical vapor deposition layer of SiN, placed between the N-polar GaN and Schottky metal, passivates surface polarization charges, and raises the barrier height by forming an amphoteric miniband structure. Optimization resulted in stable high-temperature Schottky diodes up to 400 °C.

Tang *et al.* from Xidian University investigated ferroelectric structures to flexibly manipulate certain regions along the source-drain directions of GaN transistors.<sup>23</sup> They deposited a PbZr<sub>x</sub>Ti<sub>1-x</sub>O<sub>3</sub> (PZT) film on top of the channel region of an AlGaN/GaN FET by heterogeneous integration. The electric field induced by the ferroelectric material was probed by piezoresponse force microscopy (PFM), while conducting atomic force microscopy (CAFM) was employed for detecting the resulting 2DEG distribution. Based on these findings, a ferroelectric-domain-modulated transistor was then fabricated allowing for E-mode and D-mode characteristics on the same device.

In a paper that encourages future studies of group III-nitride CMOS devices, Lu *et al.* from Xidian University report on an AlN/GaN/InGaN high electron mobility transistor (HEMT) with a steep subthreshold swing (SS) of sub-60 mV/decade. Such properties could be obtained by utilizing a "coupling-channel" architecture with two different channel regions.<sup>24</sup> The authors claim that a real-space hot carrier transfer mechanism between channel-to-gate and channel-to-channel is responsible for the very low subthreshold swing detected.

Korlacki *et al.* from University of Nebraska-Lincoln studied the effects of strain onto the direction-dependent bandgap energies in beta gallium oxide using density functional theory calculations. The authors provide sets of deformation potential parameters permitting for strain calculations on arbitrary surface orientations, for example, in pseudomorphic epitaxial growth of monoclinic-phase alloys of (AlGa)<sub>2</sub>O<sub>3</sub> or (InGa)<sub>2</sub>O<sub>3</sub>.<sup>25</sup>

In a paper highlighted by the APL editors, Duan *et al.* from Shangdong University calculated electron mobility parameters in ordered beta-phase (AlGa)<sub>2</sub>O<sub>3</sub> from first principles. Strong limitations to mobility were associated with strong polar optical phonon scattering and increasing ionicity with increasing Al content.<sup>26</sup>

Seacat *et al.* from the University of Kansas investigated electronic band structure properties of orthorhombic gallium oxide alloyed with

In and Al.<sup>27</sup> The incorporation of Al decreases the lattice constant and increases the bandgap while incorporation of In increases the lattice constants and decreases the bandgap energy suggesting wide ranges of tailoring structural and electronic properties.

On the quest for large-scale manufacturing of gallium oxide electronic devices, in a paper highlighted by the APL editors, Galazka *et al.* from Leibniz-Institut fuer Kristallzuechtung demonstrate 2-in. diameter wafer quality single crystals of the promising material, with a free electron concentration of up to  $9 \times 10^{18} \text{ cm}^{-3}$ .<sup>28</sup> High surface smoothness and stable electrical properties make these wafers excellent candidates as substrates for epitaxy and for the fabrication of vertical electronic devices.

Growth of metastable spinel-defect structure gamma-phase gallium oxide from amorphous phase was reported by Gann *et al.* from Cornell University, Ithaca.<sup>29</sup> The low surface energy of the gamma phase deduced from the results is suggested as an explanation for the often-observed gamma-phase inclusions in beta-phase gallium oxide.

In a paper highlighted by the APL editors, a solid-phase silicon suboxide (SiO) source was reported for controllable n-type doping in molecular beam epitaxy by Ardenghi *et al.* of the Paul-Drude-Institut für Festkörperelektronik. The authors further addressed concepts to reduce source oxidation during molecular beam epitaxy.<sup>30</sup>

In a paper highlighted by the APL editors, Goto *et al.* from the Tokyo University of Agriculture and Technology investigated the effect of substrate orientation on homoepitaxial growth of beta-phase gallium oxide in halide vapor phase epitaxy. Growth rate and film quality were found strongly dependent on growth orientation.<sup>31</sup>

Hilfiker *et al.* from the University of Nebraska-Lincoln reported a combined spectroscopic ellipsometry and density functional theory study of near-bandgap anisotropy of rhombohedral alpha-phase (Al<sub>x</sub>Ga<sub>1-x</sub>)<sub>2</sub>O<sub>3</sub> alloys.<sup>32</sup> Bandgap bowing parameters for the lowest individual band-to-band transitions were determined. At about 40% aluminum concentration, the bandgap changes its character from indirect in Ga<sub>2</sub>O<sub>3</sub> to direct in Al<sub>2</sub>O<sub>3</sub>.

Stokey *et al.* from the University of Nebraska-Lincoln determined the complexity of optical phonon modes in alpha-phase (AlGa)<sub>2</sub>O<sub>3</sub> alloys using infrared ellipsometry.<sup>33</sup> From their investigations, the authors also extrapolated the anisotropic static dielectric constants for the entire composition range.

Hong *et al.* from Xidian University improved gallium oxide Schottky diodes with Ni Schottky contacts by low-temperature annealing.<sup>34</sup> The diodes were fabricated on beta Ga<sub>2</sub>O<sub>3</sub> grown by hydride vapor phase epitaxy on (001) oriented Ga<sub>2</sub>O<sub>3</sub> substrate. Low temperature annealing causes a NiO formation at the Ni/Ga<sub>2</sub>O<sub>3</sub> interface and, thus, significantly reduces diode leakage current.

Zhou *et al.* from Nanjing University reported on the use of NiO as a p-type layer on Ga<sub>2</sub>O<sub>3</sub> for the fabrication of pn-diodes.<sup>35</sup> In this work, the beveled NiO layer was fabricated by applying a selective NiO regrowth technique to Ga<sub>2</sub>O<sub>2</sub> epitaxial stack on Ga<sub>2</sub>O<sub>3</sub> substrates. The diodes showed breakdown voltage levels of about 2 kV while still maintaining a comparably low on-state resistivity. The dynamic switching properties are very promising.

Hu *et al.* from Xidian University reported on optimizing Ga<sub>2</sub>O<sub>3</sub> Schottky diodes based on a W electrode by applying an oxygen plasma immediately before W deposition.<sup>36</sup> This results in the formation of tungsten-oxygen compounds as revealed by XPS. The electrical data show a much more reproducible performance on these diodes in terms of barrier height and leakage current.



Growth of metastable spinel-defect structure gamma-phase gallium oxide from amorphous phase was reported by Gann *et al.* from Cornell University, Ithaca.<sup>29</sup> The low surface energy of the gamma phase deduced from the results is suggested as an explanation for the often-observed gamma-phase inclusions in beta-phase gallium oxide.

Dela Cruz *et al.* from the University of Canterbury investigated *in situ* oxidized platinum/iridium Schottky contacts on Ga<sub>2</sub>O<sub>3</sub> with the goal to realize near ideal, low leakage Schottky interfaces to Ga<sub>2</sub>O<sub>3</sub>.<sup>37</sup> The oxidized metals were realized by Ir and Pt co-sputtering in oxygen-argon environment. This method allows for an exact control of the respective contact oxidation state. Optimum contacts show ideality factor near unity and a barrier height of 2 eV. The Schottky properties are nearly independent of the Ga<sub>2</sub>O<sub>3</sub> crystal orientation.

The nano-scale integration of beta-Ga<sub>2</sub>O<sub>3</sub> with N-face GaN can potentially enable the fabrication of novel GaN/Ga<sub>2</sub>O<sub>3</sub> high-frequency and high-power devices combining the merits of both GaN and Ga<sub>2</sub>O<sub>3</sub> in addition to novel optoelectronic devices. This concept was pursued by Jian *et al.* from the University of Michigan.<sup>38</sup> Hydrophilic bonds due to special chemical treatment of the surfaces followed by an annealing step provided the targeted atomical bonding without any loss in crystalline quality.

Vertical Ga<sub>2</sub>O<sub>3</sub> power switching devices require rather thick Ga<sub>2</sub>O<sub>3</sub> layers with high crystalline quality. Saha *et al.* from the University at Buffalo investigated Ga<sub>2</sub>O<sub>3</sub> films grown by low-pressure vapor phase epitaxy at 1050 °C and with growth rates between 13 and 19 μm/h.<sup>39</sup> The Schottky characteristics of the up to 21 μm thick epitaxial layers were characterized. It was found that the macro-scale roughness of the layers is more decisive for performance as compared to the root mean square surface roughness.

In a paper highlighted by the APL editors, Tetzner *et al.* from the Leibniz-Institut für Hochfrequenztechnik described a new method of using a molecular beam epitaxy SnO layer for creating a p-n junction underneath the gate electrode and, thus, to provide means for releasing normally-off Ga<sub>2</sub>O<sub>3</sub> transistors using this approach.<sup>40</sup> On ⟨100⟩ oriented Ga<sub>2</sub>O<sub>3</sub> material, a p-type concentration of  $7 \times 10^{18}/\text{cm}^3$  at a hole mobility of 1.5 cm<sup>2</sup>/V s could be achieved. Therefore, this technology is feasible and can, in principle, be extended toward normally off devices or used for p-type guard rings for high voltage applications.

Xu *et al.* from the Chinese Academy of Sciences, Beijing, demonstrated a Ga<sub>2</sub>O<sub>3</sub> FinFET in a 60-nm-wide nanowire configuration controlled by a tri-gate structure.<sup>41</sup> The FinFET performance is characterized by extremely low leakage, very high turn on/off ratio, and a nearly optimum subthreshold voltage swing of 110 mV/decade.

A p-NiO<sub>x</sub> edge termination with the field plate structure and low interface trap density in n-type β-Ga<sub>2</sub>O<sub>3</sub> for a Schottky barrier diode was demonstrated by Yan *et al.* from Xidian University.<sup>42</sup> A high performance diode with a power figure of merit of 1.11 GW/cm<sup>2</sup> and forward current/break down voltage > 7 A/1200 V was reported offering a great promise for next generation high power switching applications.

Probe-induced surface defects and strain causing a reverse leakage current path were investigated in gallium oxide Schottky barrier diodes by Sdoeung *et al.* from Saga University.<sup>43</sup> Each defect corresponds to a reverse leakage current of  $-0.725 \mu\text{A}$  at a reverse bias of  $-140 \text{ V}$ , and a probe-induced pressure of 0.206 GPa created surface defects along with a reverse leakage current of  $-3.75 \text{ nA}$  at a reverse voltage of  $-140 \text{ V}$ .

Fregolent *et al.* from the University of Padova proposed a trapping and detrapping model for traps close to the Al<sub>2</sub>O<sub>3</sub>/β-Ga<sub>2</sub>O<sub>3</sub> interface in lateral MOSFETs with Al<sub>2</sub>O<sub>3</sub> gate dielectrics.<sup>44</sup> An innovative fast C–V experimental setup and an inhibition model that includes the repulsive effects onto trapped carriers is considered for both trap filling and emission processes.

Saha *et al.* from University at Buffalo analyzed the influence of *ex situ* passivation on the dynamic performance of β-(Al<sub>x</sub>Ga<sub>1-x</sub>)<sub>2</sub>O<sub>3</sub>/Ga<sub>2</sub>O<sub>3</sub> hetero-structure FETs (HFETs).<sup>45</sup> The investigations were performed before and after silicon nitride (Si<sub>3</sub>N<sub>4</sub>) passivation. The device showed moderate current collapse after passivation, however, pronounced differences between DC and pulsed operation due to self-heating.

Sdoeung *et al.* of Saga University analyzed line shape defects in halide vapor phase epitaxy grown Ga<sub>2</sub>O<sub>3</sub> epitaxial layers intended for the fabrication of Schottky diodes.<sup>46</sup> The authors demonstrated that line shape defects originating from the ⟨100⟩ Ga<sub>2</sub>O<sub>3</sub> substrate are acting as additional leakage current paths in the drift zone of Schottky diodes.

This section groups articles on novel wide bandgap materials that need to be analyzed by theory and experiment to explore possible applications for rf- and power electronics. In this context, boron nitride is an emerging material with strong potential for power and rf-electronics due to its wide bandgap and its pronounced thermal conductivity.

Chilleri *et al.* at the New Mexico Institute of Mining and Technology provide an overview on the prospective properties of cubic boron nitride.<sup>47</sup> Calculations predict that electrons can reach high saturation velocities at high electric fields. Among other properties, the high saturation velocity renders the material interesting for high power rf-applications. Compared with established competitive semiconductors, it was shown that BN offers an advantage in terms of cutoff frequency fit as a function of transistor gate length.

In a paper highlighted by the APL editors, Turiansky *et al.* from the University of California, Santa Barbara, provided first-principles calculations on the possibility to n-type dope cubic BN. The hybrid density functional theory results addressed potential n-type dopants and compensating centers in c-BN.<sup>48</sup> Accordingly, Si dopants on boron lattice sites and oxygen dopants on nitrogen sites are considered as very promising for future BN technologies as these dopants are not impacted by self-compensation effects. This opens the potential for subsequent technology developments toward n-type doped BN devices.

Moret *et al.* from the Center National de la Recherche Scientifique, Université de Montpellier, reported on growth of rhombohedral and turbostratic boron nitride by metal organic vapor deposition.<sup>49</sup> Structural and optical signatures were verified by x-ray diffraction and photoluminescence investigations.

Ng *et al.* from Singapore University of Technology and Design analyzed the tuning capabilities of two-dimensional van der Waals heterostructures based on MoSi<sub>2</sub>N<sub>4</sub> wideband heterostructures on GaN and ZnO.<sup>50</sup> Among others, the authors found that the application of an external perpendicular electric field or mechanical strain effectively alters the bandgap type and the band alignment type of the heterostructures, thus offering an interesting tuning knob for engineering the electronic and optoelectronic properties of such heterostructures for future device application.

Hilfiker *et al.* from the University of Nebraska-Lincoln reported on the elevated temperature shifts of the excitonic properties and bandgap energies in the emergent ultrawide bandgap semiconductor ZnGa<sub>2</sub>O<sub>4</sub>.<sup>51</sup> A strong excitonic binding energy and exciton evaporation at higher temperature was observed.

Wu *et al.* at Fudan University investigated shear-horizontal (SH) surface acoustic wave (SAW) resonators on YX-LiNbO<sub>3</sub>/SiO<sub>2</sub>/Si substrates with 30° orientation.<sup>52</sup> The authors demonstrated structures with high electro-mechanical coupling factor  $k_{\text{eff}}^2$  of 24 along with high Bode-Q<sub>max</sub> quality factor of 1107. This makes material and technology suitable for wideband tuning filter applications as required in modern communication systems.

Matsumoto *et al.* at Kanazawa University developed a normally off inversion p-channel metal-oxide-semiconductor field-effect transistor (MOSFET) on top of a nitrogen (N)-doped diamond body.<sup>53</sup> The nitrogen doping was realized by microwave plasma-enhanced chemical vapor deposition with intention to replace the currently often used phosphorus (P) doping and reduce environmental fabrication risks of diamond devices. The results are compared to phosphorus doped diamond.

Ren *et al.* at Xidian University developed a double-stack MoO<sub>3</sub>/Si<sub>3</sub>N<sub>4</sub> gate dielectric layer for diamond transistors fabricated on hydrogen terminated diamond surfaces.<sup>54</sup> Compared to a single stack, the robustness of the gate could be enhanced. This results in improved operation characteristics of the diamond FETs. For example, a drain current level of about 120 mA/mm was obtained.

In a featured paper, Ghosh *et al.* from the University of California, Riverside, analyzed the noise behavior of vertical high-current diamond diodes.<sup>55</sup> The intention of the authors was to develop noise spectroscopy-based approaches for device reliability assessment. In high turn-on voltage diodes, the 1/f noise dominates and can be attributed to the higher concentration of traps. In contrast, the generation recombination (G-R) noise was found to be characteristic of diamond diodes with lower turn-on voltages.

Yang *et al.* from Arizona State University reported on a thin layer of Al<sub>2</sub>O<sub>3</sub> introduced as an interfacial layer between the surface conductive hydrogen-terminated (H-terminated) diamond and the MoO<sub>3</sub> electrode.<sup>56</sup> Thereby, the authors increased the distance between the hole accumulation layer in diamond and the negatively charged states in the acceptor layer. This reduces Coulomb scattering in the hole channel region and, therefore, increases hole mobility.

He *et al.* from Xi'an Jiaotong University reported on hydrogen terminated diamond transistors.<sup>57</sup> The authors developed a spin-on SnO<sub>2</sub> film for acting as an efficient gate insulator before depositing the Al gate electrode. The spin-on SnO<sub>2</sub> layers are p-type, repel holes in the 2DHG layer, and provide normally off drive conditions.

Surdi *et al.* from Arizona State University provide improved theoretical understanding for figure of merit (FOM) calculations in diamond-based diodes.<sup>58</sup> An interpretation of the unipolar FOM based on the Mott-Gurney square law is discussed in comparison with the traditional Ohmic-based FOM. Silvaco simulations were found to be in excellent agreement with the analytically derived Mott-Gurney parameters for low-doped punch-through diodes.

Woo *et al.* from Stanford University studied various diamond structures for extrinsic photoconductive semiconductor switches.<sup>59</sup> Photo responses were measured at electric fields of 3.3–33 kV/cm. A highest average on/off-state current ratio on the order of 10<sup>11</sup> was reported. Boron containing devices showed appreciable response to illumination with 1064 nm.

Wu *et al.* from Xidian University studied structural and thermal properties of polycrystalline diamond thin films grown on GaN-on-SiC.<sup>60</sup> Strain variations are assessed by Raman spectroscopy and thermal properties are extracted by time domain thermoreflectance.

Device simulations suggest improvement of thermal boundary resistance and strain increase the 2DEG density by nearly 5%.

Hou *et al.* from Chinese Academy of Sciences Changchun reported on structural, optical, electronic, and optoelectronic properties of MgGa<sub>2</sub>O<sub>4</sub> thin films grown by using metal organic chemical vapor deposition on the c-plane sapphire.<sup>61</sup> Solar-blind ultraviolet photodetection characteristics and annealing effects in oxygen are discussed for this material with a bandgap of 5.18 eV.

Enhancement of the deep ultraviolet photoresponse of a h-BN device coupled with plasmonic nanostructures was reported by Zhu *et al.* from Jilin University.<sup>62</sup> The photocurrent is enhanced 7–9 times under the illumination of 205 nm with a cutoff wavelength of approximately 220 nm.

Yang *et al.* from University of Science and Technology of China Hefei discuss competing processes between the generation and recombination rate of photo-induced carriers in AlGaIn/GaN-based ultraviolet phototransistor at room and high temperatures.<sup>63</sup>

Muthuraj *et al.* from University of California Santa Barbara showed a record high light output power for N-polar LEDs, up to 0.21 mW on-wafer at 20 A/cm<sup>2</sup> with an emission wavelength of 470 nm. The N-polar InGaIn LEDs with an inverted p-side down configuration and buried tunnel junctions were grown by metalorganic chemical vapor deposition.<sup>64</sup>

Chen *et al.* from South China University of Technology Guangzhou investigated the electronic and optical properties of GeS<sub>2</sub>/GaN heterojunctions by experiments and first-principles calculations.<sup>65</sup> Fast rise and fall times of <0.30 and 1.10 ms, respectively, were determined for 365 nm excitation and the potential for use in high performance, self-powered ultraviolet photodetection was highlighted.

Han *et al.* from Songshan Lake Materials Laboratory Dongguan presented magnetron-sputtered indium gallium zinc oxide/amorphous gallium oxide ultraviolet photodetector structures with promising performance parameters including high on/off ratio and field-effect mobility of ~10<sup>8</sup> and 8.3 cm<sup>2</sup>/V s, respectively.<sup>66</sup> The simple and low-cost fabrication process may be suitable for large-area active-matrix photodetector arrays.

In a paper highlighted by the APL editors, *in situ* temperature measurements of the channel temperature for a gallium oxide MOSFET were demonstrated by Zheng *et al.* from the University of Bristol.<sup>67</sup> A trapping tolerant method was proposed introducing a pre-trapping process to minimize the effect of trapping onto temperature measurements.

Yao *et al.* from Chinese Academy of Sciences Beijing reported on capacitance-mode deep-level transient spectroscopy characterization of trap characteristics in AlGaIn/GaN metal-insulator-semiconductor high electron mobility transistors with SiN<sub>x</sub> as gate insulator.<sup>68</sup> Two distinctive trap-emission transients were observed and associated with states at the SiN<sub>x</sub>/AlGaIn interface and bulk states from the SiN<sub>x</sub> where the latter become charged at large overdrive voltages leading to severe threshold voltage instability.

Chang *et al.* from Peking University Shenzhen Graduate School proposed a model for analysis of properties of deep defects from electrical measurements in GaN. Structural and optical investigations further indicated support for the proposed model. However, a comment on the work of Chang *et al.*<sup>69</sup> was made by Thonke from Ulm University pointing out a potential error in photoluminescence analysis due to instrumentation induced artifacts.<sup>70</sup>

Two letters report on measurement of two-dimensional electron gas (2DEG).

Kuehne *et al.* from Linköping University performed THz optical Hall effect measurements on an AlN/Al<sub>x</sub>Ga<sub>1-x</sub>N transistor structure with a high aluminum content ( $x = 0.78$ ).<sup>71</sup> The experimental 2DEG mobility in the channel is found within the expected range; the effective mass of 2DEG electrons at low temperatures, however, was found nearly twice as large than the respective bulk value.

Wang *et al.* from Cornell University, Ithaca, demonstrate the use of a scanning microwave microscope to measure the sheet resistance of 2D electron or hole gas (2DEG or 2DHG) at the interface of an AlN/GaN heterostructure.<sup>72</sup>

Both letters illustrate the progress made in contact-free and non-destructive measurements of electrical properties of semiconductor heterostructures.

Schubert *et al.* from the University of Nebraska-Lincoln reported on a novel approach to terahertz (THz) electron paramagnetic resonance generalized spectroscopic ellipsometry (THz-EPR-GSE) measurements of field and frequency dependencies of spin transitions associated with the nitrogen defect in 4H-SiC.<sup>73</sup> The new method permits convenient experimental measurements to defect-related spin densities in homo and heteroepitaxial semiconductor material systems and improves sensitivity over traditional EPR approaches.

Single-event burnout (SEB) considerably impedes high-power device operation in radiation-exposed environment. To better understand the mechanisms limiting radiation hardness, McPherson *et al.* from Rensselaer Polytechnic Institute explored and elucidated physical failure mechanisms caused by single heavy ion strikes in high voltage 4H-SiC superjunction (SJ) vertical DMOSFETs.<sup>74</sup> The authors simulated the devices and evidenced that SJ type SiC DMOSFETs outperform non-SJ SiC devices by a factor of 2.2 in terms of the survival threshold voltage. In all cases, BEB degradation mechanism is caused by local mesoplasma formation and, thus, excessive heating in certain device regions.

Liu *et al.* from Xidian University investigated how trap states in GaN/AlGaIn transistors with AlN/GaN superlattice channel on Si substrates are generated and modified during on-going ionizing gamma radiation.<sup>75</sup> Frequency-dependent capacitance and conductance measurements were used to analyze the evolution of gamma irradiation onto trap states in the electron channel. Irradiation induces acceptor-like trap states in the lower superlattice channel and that compensate electrons there.

In a featured paper, Shimbori and Huang from University of Texas at Austin consider design methodology and fabrication of 4H-SiC lateral RESURF Schottky diodes, using thin RESURF layer epitaxial wafers.<sup>76</sup> The fabricated lateral devices demonstrated competitive performance, which can be further enhanced by the edge termination structures proposed.

M.S. acknowledges the support by NSF under Award No. OIA-2044049 RII Track-1: Emergent Quantum Materials and Technologies (EQUATE); by the Air Force Office of Scientific Research under Award Nos. FA9550-19-S-0003, FA9550-21-1-0259, and FA9550-23-1-0574 DEE; and by the University of Nebraska Foundation, and by the J.A. Woollam Foundation. H.G.X. acknowledges partial support from the Japan Science and Technology Agency (JST) as part of Advanced International Collaborative Research Program (AdCORP), Grant Number JPMJKB2303.

## REFERENCES

- J. Park *et al.*, “N<sub>2</sub>O plasma treatment effect on reliability of p-GaN gate AlGaIn/GaN HEMTs,” *Appl. Phys. Lett.* **120**, 132103 (2022).
- J. Chen *et al.*, “Study of minority carrier traps in p-GaN gate HEMT by optical deep level transient spectroscopy,” *Appl. Phys. Lett.* **120**, 212105 (2022).
- E. S. Lee, J. Joh, D. S. Lee, and J. A. del Alamo, “Gate-geometry dependence of electrical characteristics of p-GaN gate HEMTs,” *Appl. Phys. Lett.* **120**, 082104 (2022).
- M. Rahman, N. Kalarickal, H. Lee, T. Razzak, and S. Rajan, “Integration of high permittivity BaTiO<sub>3</sub> with AlGaIn/GaN for near-theoretical breakdown field kV-class transistors,” *Appl. Phys. Lett.* **119**, 193501 (2021).
- K. Shima *et al.*, “Improved minority carrier lifetime in p-type GaN segments prepared by vacancy-guided redistribution of Mg,” *Appl. Phys. Lett.* **119**, 182106 (2021).
- Y. Liao *et al.*, “Improved device performance of vertical GaN-on-GaN nanorod Schottky barrier diodes with wet-etching process,” *Appl. Phys. Lett.* **120**, 122109 (2022).
- K. Nomoto *et al.*, “Distributed polarization-doped GaN p-n diodes with near-unity ideality factor and avalanche breakdown voltage of 1.25 kV,” *Appl. Phys. Lett.* **120**, 122111 (2022).
- R. Zhu, H. Jiang, C. Tang, and K. Lau, “Vertical GaN trench MOSFETs with step-graded channel doping,” *Appl. Phys. Lett.* **120**, 242104 (2022).
- P. C. Shih, Z. Engel, H. Ahamad, W. A. Doolittle, and T. Palacios, “Wet-based digital etching on GaN and AlGaIn,” *Appl. Phys. Lett.* **120**, 022101 (2022).
- S. DasGupta *et al.*, “Identification of the defect dominating high temperature reverse leakage current in vertical GaN power diodes through deep level transient spectroscopy,” *Appl. Phys. Lett.* **120**, 053502 (2022).
- K. Mukherjee *et al.*, “Study and characterization of GaN MOS capacitors: Planar vs trench topographies,” *Appl. Phys. Lett.* **120**, 143501 (2022).
- L. Nela, M. Xiao, Y. Zhang, and E. Matioli, “A perspective on multi-channel technology for the next-generation of GaN power devices,” *Appl. Phys. Lett.* **120**, 190501 (2022).
- Y. Zhou *et al.*, “High performance millimeter-wave InAlN/GaN HEMT for low voltage RF applications via regrown Ohmic contact with contact ledge structure,” *Appl. Phys. Lett.* **120**, 062104 (2022).
- P. Wang *et al.*, “Demonstration of 16 THz V Johnson’s figure-of-merit and 36 THz V f<sub>max</sub>-V<sub>BE</sub> in ultrathin barrier AlGaIn/GaN HEMTs with slant-field-plate T-gates,” *Appl. Phys. Lett.* **120**, 102103 (2022).
- H. Ye, M. Gaevski, G. Simin, A. Khan, and P. Fay, “Electron mobility and velocity in Al<sub>0.45</sub>Ga<sub>0.55</sub>N-channel ultra-wide bandgap HEMTs at high temperatures for RF power applications,” *Appl. Phys. Lett.* **120**, 103505 (2022).
- S. Ghosh *et al.*, “Low-frequency noise characteristics of GaN vertical PIN diodes—Effects of design, current, and temperature,” *Appl. Phys. Lett.* **119**, 243505 (2021).
- Z. Zhang *et al.*, “Polarization-induced 2D hole gases in pseudomorphic undoped GaN/AlN heterostructures on single-crystal AlN substrates,” *Appl. Phys. Lett.* **119**, 162104 (2021).
- A. Krishna *et al.*, “Acceptor traps as the source of holes in p-type N-polar GaN/AlN/AlGaIn superlattices,” *Appl. Phys. Lett.* **120**, 132104 (2022).
- Z. Zheng, T. Chen, L. Zhang, W. Song, and K. Chen, “Unveiling the parasitic electron channel under the gate of enhancement-mode p-channel GaN field-effect transistors on the p-GaN/AlGaIn/GaN platform,” *Appl. Phys. Lett.* **120**, 152102 (2022).
- H. Su *et al.*, “Mechanism of low Ohmic contact resistance to p-type GaN by suppressed edge dislocations,” *Appl. Phys. Lett.* **120**, 222101 (2022).
- D. Khachariya *et al.*, “Record >10 MV/cm mesa breakdown fields in Al<sub>0.85</sub>Ga<sub>0.15</sub>N/Al<sub>0.6</sub>Ga<sub>0.4</sub>N high electron mobility transistors on native AlN substrates,” *Appl. Phys. Lett.* **120**, 172106 (2022).
- D. Khachariya *et al.*, “Schottky contacts to N-polar GaN with SiN interlayer for elevated temperature operation,” *Appl. Phys. Lett.* **120**, 172109 (2022).
- X. Tang *et al.*, “Ferroelectric domain modulated AlGaIn/GaN field effect transistor,” *Appl. Phys. Lett.* **120**, 035503 (2022).
- H. Lu *et al.*, “AlN/GaN/InGaIn coupling-channel HEMTs with steep subthreshold swing of sub-60 mV/decade,” *Appl. Phys. Lett.* **120**, 173502 (2022).
- R. Korlacki *et al.*, “Linear strain and stress potential parameters for the three fundamental band to band transitions in  $\beta$ -Ga<sub>2</sub>O<sub>3</sub>,” *Appl. Phys. Lett.* **120**, 042103 (2022).
- X. Duan, T. Wang, Z. Fu, J.-Y. Yang, and L. Liu, “Electron mobility in ordered  $\beta$ -(Al<sub>x</sub>Ga<sub>1-x</sub>)<sub>2</sub>O<sub>3</sub> alloys from first-principles,” *Appl. Phys. Lett.* **121**, 042103 (2022).
- S. Seacat, J. Lyons, and H. Peelaers, “Properties of orthorhombic Ga<sub>2</sub>O<sub>3</sub> alloyed with In<sub>2</sub>O<sub>3</sub> and Al<sub>2</sub>O<sub>3</sub>,” *Appl. Phys. Lett.* **119**, 042104 (2021).



- <sup>28</sup>Z. Galazka *et al.*, "Two inch diameter, highly conducting bulk  $\beta$ -Ga<sub>2</sub>O<sub>3</sub> single crystals grown by the Czochralski method," *Appl. Phys. Lett.* **120**, 152101 (2022).
- <sup>29</sup>K. R. Gann *et al.*, "Initial nucleation of metastable  $\gamma$ -Ga<sub>2</sub>O<sub>3</sub> during sub-millisecond thermal anneals of amorphous Ga<sub>2</sub>O<sub>3</sub>," *Appl. Phys. Lett.* **121**, 062102 (2022).
- <sup>30</sup>A. Ardenghi *et al.*, "Toward controllable Si-doping in oxide molecular beam epitaxy using a solid SiO source: Application to  $\beta$ -Ga<sub>2</sub>O<sub>3</sub>," *Appl. Phys. Lett.* **121**, 042109 (2022).
- <sup>31</sup>K. Goto *et al.*, "Effect of substrate orientation on homoepitaxial growth of  $\beta$ -Ga<sub>2</sub>O<sub>3</sub> by halide vapor phase epitaxy," *Appl. Phys. Lett.* **120**, 102102 (2022).
- <sup>32</sup>M. Hilfiker *et al.*, "Anisotropic dielectric function, direction dependent bandgap energy, band order, and indirect to direct gap crossover in  $\alpha$ -(Al<sub>x</sub>Ga<sub>1-x</sub>)<sub>2</sub>O<sub>3</sub> (0 ≤ x ≤ 1)," *Appl. Phys. Lett.* **121**, 052101 (2022).
- <sup>33</sup>M. Stokey *et al.*, "Infrared-active phonon modes and static dielectric constants in  $\alpha$ -(Al<sub>x</sub>Ga<sub>1-x</sub>)<sub>2</sub>O<sub>3</sub> (0.18 ≤ x ≤ 0.54) alloys," *Appl. Phys. Lett.* **120**, 112202 (2022).
- <sup>34</sup>Y. Hong *et al.*, "The optimized interface characteristics of  $\beta$ -Ga<sub>2</sub>O<sub>3</sub> Schottky barrier diode with low temperature annealing," *Appl. Phys. Lett.* **119**, 132103 (2021).
- <sup>35</sup>F. Zhou *et al.*, "Over 1.8 GW/cm<sup>2</sup> beveled-mesa NiO/ $\beta$ -Ga<sub>2</sub>O<sub>3</sub> heterojunction diode with 800 V/10 A nanosecond switching capability," *Appl. Phys. Lett.* **119**, 262103 (2021).
- <sup>36</sup>H. Hu *et al.*, "The role of surface pretreatment by low temperature O<sub>2</sub> gas annealing for  $\beta$ -Ga<sub>2</sub>O<sub>3</sub> Schottky barrier diodes," *Appl. Phys. Lett.* **120**, 073501 (2022).
- <sup>37</sup>Z. Dela Cruz, C. Hou, R. Martinez-Gazoni, R. Reeves, and M. Allen, "Performance of in situ oxidized platinum/iridium alloy Schottky contacts on (001), (201), and (010)  $\beta$ -Ga<sub>2</sub>O<sub>3</sub>," *Appl. Phys. Lett.* **120**, 083503 (2022).
- <sup>38</sup>Z. Jian, C. Clymore, K. Sun, U. Mishra, and E. Ahmadi, "Demonstration of atmospheric plasma activated direct bonding of N-polar GaN and  $\beta$ -Ga<sub>2</sub>O<sub>3</sub> (001) substrates," *Appl. Phys. Lett.* **120**, 142101 (2022).
- <sup>39</sup>S. Saha *et al.*, "Schottky diode characteristics on high-growth rate LPCVD  $\beta$ -Ga<sub>2</sub>O<sub>3</sub> films on (010) and (001) Ga<sub>2</sub>O<sub>3</sub> substrates," *Appl. Phys. Lett.* **120**, 122106 (2022).
- <sup>40</sup>K. Tetzner *et al.*, "SnO/ $\beta$ -Ga<sub>2</sub>O<sub>3</sub> heterojunction field-effect transistors and vertical p-n diodes," *Appl. Phys. Lett.* **120**, 112110 (2022).
- <sup>41</sup>S. Xu *et al.*, "Single  $\beta$ -Ga<sub>2</sub>O<sub>3</sub> nanowire based lateral FinFET on Si," *Appl. Phys. Lett.* **120**, 153501 (2022).
- <sup>42</sup>Q. Yan *et al.*, "Low density of interface trap states and temperature dependence study of Ga<sub>2</sub>O<sub>3</sub> Schottky barrier diode with p-NiO<sub>x</sub> termination," *Appl. Phys. Lett.* **120**, 092106 (2022).
- <sup>43</sup>S. Sdoeung *et al.*, "Probe-induced surface defects: Origin of leakage current in halide vapor-phase epitaxial (001)  $\beta$ -Ga<sub>2</sub>O<sub>3</sub> Schottky barrier diodes," *Appl. Phys. Lett.* **120**, 092101 (2022).
- <sup>44</sup>M. Fregolent *et al.*, "Logarithmic trapping and detrapping in  $\beta$ -Ga<sub>2</sub>O<sub>3</sub> MOSFETs: Experimental analysis and modeling," *Appl. Phys. Lett.* **120**, 163502 (2022).
- <sup>45</sup>C. Saha, A. Vaidya, and U. Singiseti, "Temperature dependent pulsed IV and RF characterization of  $\beta$ -(Al<sub>x</sub>Ga<sub>1-x</sub>)<sub>2</sub>O<sub>3</sub>/Ga<sub>2</sub>O<sub>3</sub> hetero-structure FET with ex situ passivation," *Appl. Phys. Lett.* **120**, 172102 (2022).
- <sup>46</sup>S. Sdoeung *et al.*, "Line-shaped defects: Origin of leakage current in halide vapor-phase epitaxial (001)  $\beta$ -Ga<sub>2</sub>O<sub>3</sub> Schottky barrier diodes," *Appl. Phys. Lett.* **120**, 122107 (2022).
- <sup>47</sup>J. Chilleri, P. Siddiqua, M. Shur, and S. O'Leary, "Cubic boron nitride as a material for future electron device applications: A comparative analysis," *Appl. Phys. Lett.* **120**, 122105 (2022).
- <sup>48</sup>M. Turiansky, D. Wickramaratne, J. Lyons, and C. Van de Walle, "Prospects for n-type conductivity in cubic boron nitride," *Appl. Phys. Lett.* **119**, 162105 (2021).
- <sup>49</sup>M. Moret *et al.*, "Rhombohedral and turbostratic boron nitride: X-ray diffraction and photoluminescence signatures," *Appl. Phys. Lett.* **119**, 262102 (2021).
- <sup>50</sup>J. Ng, Q. Wu, L. Ang, and Y. Ang, "Tunable electronic properties and band alignments of MoSi<sub>2</sub>N<sub>4</sub>/GaN and MoSi<sub>2</sub>N<sub>4</sub>/ZnO van der Waals heterostructures," *Appl. Phys. Lett.* **120**, 103101 (2022).
- <sup>51</sup>M. Hilfiker *et al.*, "Elevated temperature spectroscopic ellipsometry analysis of the dielectric function, exciton, band-to-band transition, and high-frequency dielectric constant properties for single-crystal ZnGa<sub>2</sub>O<sub>4</sub>," *Appl. Phys. Lett.* **120**, 132105 (2022).
- <sup>52</sup>S. Wu *et al.*, "High-performance SH-SAW resonator using optimized 30° YX-LiNbO<sub>3</sub>/SiO<sub>2</sub>/Si," *Appl. Phys. Lett.* **120**, 242201 (2022).
- <sup>53</sup>T. Matsumoto *et al.*, "Fabrication of inversion p-channel MOSFET with a nitrogen-doped diamond body," *Appl. Phys. Lett.* **119**, 242105 (2021).
- <sup>54</sup>Z. Ren *et al.*, "Diamond MOSFET with MoO<sub>3</sub>/Si<sub>3</sub>N<sub>4</sub> doubly stacked gate dielectric," *Appl. Phys. Lett.* **120**, 042104 (2022).
- <sup>55</sup>S. Ghosh *et al.*, "Excess noise in high-current diamond diodes," *Appl. Phys. Lett.* **120**, 062103 (2022).
- <sup>56</sup>Y. Yang, F. Koeck, X. Wang, and R. Nemanich, "Surface transfer doping of MoO<sub>3</sub> on hydrogen terminated diamond with an Al<sub>2</sub>O<sub>3</sub> interfacial layer," *Appl. Phys. Lett.* **120**, 191602 (2022).
- <sup>57</sup>S. He *et al.*, "Solution-processed tin oxide thin film for normally-off hydrogen terminated diamond field effect transistor," *Appl. Phys. Lett.* **120**, 132102 (2022).
- <sup>58</sup>H. Surdi, T. Thornton, R. Nemanich, and S. Goodnick, "Space charge limited corrections to the power figure of merit for diamond," *Appl. Phys. Lett.* **120**, 223503 (2022).
- <sup>59</sup>K. Woo, M. Malakoutian, B. Reeves, and S. Chowdhury, "A study on sub-bandgap photoexcitation in nitrogen- and boron-doped diamond with interdigitated device structure," *Appl. Phys. Lett.* **120**, 112104 (2022).
- <sup>60</sup>M. Wu *et al.*, "Structural and thermal analysis of polycrystalline diamond thin film grown on GaN-on-SiC with an interlayer of 20 nm PECVD-SiN," *Appl. Phys. Lett.* **120**, 121603 (2022).
- <sup>61</sup>Q. Hou *et al.*, "MOCVD growth of MgGa<sub>2</sub>O<sub>4</sub> thin films for high-performance solar-blind UV photodetectors," *Appl. Phys. Lett.* **120**, 011101 (2022).
- <sup>62</sup>X. Zhu *et al.*, "Plasmonic enhancement in deep ultraviolet photoresponse of hexagonal boron nitride thin films," *Appl. Phys. Lett.* **120**, 091109 (2022).
- <sup>63</sup>L. Yang *et al.*, "Temperature-dependent photodetection behavior of AlGaN/GaN-based ultraviolet phototransistors," *Appl. Phys. Lett.* **120**, 091103 (2022).
- <sup>64</sup>V. Muthuraj *et al.*, "Inverted N-polar blue and blue-green light emitting diodes with high power grown by metalorganic chemical vapor deposition," *Appl. Phys. Lett.* **120**, 101104 (2022).
- <sup>65</sup>S. Chen *et al.*, "Large-scale m-GeSe grown on GaN for self-powered ultrafast UV photodetection," *Appl. Phys. Lett.* **120**, 111101 (2022).
- <sup>66</sup>Z. Han *et al.*, "High-performance IGZO/Ga<sub>2</sub>O<sub>3</sub> dual-active-layer thin film transistor for deep UV detection," *Appl. Phys. Lett.* **120**, 262102 (2022).
- <sup>67</sup>X. Zheng, T. Moule, J. Pomeroy, M. Higashiwaki, and M. Kuball, "A trapping tolerant drain current based temperature measurement of  $\beta$ -Ga<sub>2</sub>O<sub>3</sub> MOSFETs," *Appl. Phys. Lett.* **120**, 073502 (2022).
- <sup>68</sup>Y. Yao *et al.*, "Identification of bulk and interface state-induced threshold voltage instability in metal/SiN<sub>x</sub>(insulator)/AlGaN/GaN high-electron-mobility transistors using deep-level transient spectroscopy," *Appl. Phys. Lett.* **119**, 233502 (2021).
- <sup>69</sup>K. Chang *et al.*, "The observation of Gaussian distribution and origination identification of deep defects in AlGaN/GaN MIS-HEMT," *Appl. Phys. Lett.* **120**, 172107 (2022).
- <sup>70</sup>K. Thonke, "Comment on 'The observation of Gaussian distribution and origination identification of deep defects in AlGaN/GaN MIS-HEMT' [Appl. Phys. Lett. **120**, 172107 (2022)]," *Appl. Phys. Lett.* **121**, 066101 (2022).
- <sup>71</sup>P. Kuehne *et al.*, "Enhancement of 2DEG effective mass in AlN/Al<sub>0.78</sub>Ga<sub>0.22</sub>N high electron mobility transistor structure determined by THz optical Hall effect," *Appl. Phys. Lett.* **120**, 253102 (2022).
- <sup>72</sup>X. Wang *et al.*, "Quantitative scanning microwave microscopy of 2D electron and hole gases in AlN/GaN heterostructures," *Appl. Phys. Lett.* **120**, 012103 (2022).
- <sup>73</sup>M. Schubert *et al.*, "Terahertz electron paramagnetic resonance generalized spectroscopic ellipsometry: The magnetic response of the nitrogen defect in 4H-SiC," *Appl. Phys. Lett.* **120**, 102101 (2022).
- <sup>74</sup>J. McPherson, A. Woodworth, T. Chow, and W. Ji, "Simulation-based study of single-event burnout in 4H-SiC high-voltage vertical superjunction DMOSFET: Physical failure mechanism and robustness vs performance tradeoffs," *Appl. Phys. Lett.* **120**, 043501 (2022).
- <sup>75</sup>S. Liu *et al.*, "Characterization of trap states in AlN/GaN superlattice channel high electron mobility transistors under total-ionizing-dose with <sup>60</sup>Co  $\gamma$ -irradiation," *Appl. Phys. Lett.* **120**, 202102 (2022).
- <sup>76</sup>A. Shimbori and A. Huang, "Design methodologies and fabrication of 4H-SiC lateral Schottky barrier diode on thin RESURF layer," *Appl. Phys. Lett.* **120**, 122103 (2022).